2026, 66(8): 4097-4118
CSTR: 32112.14.j.AMS.20260134
DOI: 10.13343/j.cnki.wsxb.20260134

微生物学报
Acta Microbiologica Sinica
http://journals.im.ac.cn/actamicrocn

Research Article 研究报告

代谢改造酿酒酵母合成麦角硫因

赛尔曼，李肖肖，杨群，赵运英*，邓禹*

江南大学 生物工程学院，工业生物技术教育部重点实验室，江苏 无锡

赛尔曼, 李肖肖, 杨群, 赵运英, 邓禹. 代谢改造酿酒酵母合成麦角硫因[J]. 微生物学报, 2026, 66(8): 4097-4118.
Khan Salman, LI Xiaoxiao, YANG Qun, ZHAO Yunying, DENG Yu. Metabolic engineering of *Saccharomyces cerevisiae* for the production of ergothioneine[J]. Acta Microbiologica Sinica, 2026, 66(8): 4097-4118.

摘　要：【目的】麦角硫因(ergothioneine, EGT)是一种含硫组氨酸衍生物，被广泛应用于食品、制药及化妆品领域。然而，由于传统化学合成法和提取法成本高昂且效率低下，EGT 的工业化生产受到严重制约。本研究旨在以酿酒酵母为底盘细胞构建生物合成 EGT 的微生物细胞工厂。【方法】通过在酿酒酵母中异源表达来自粗糙脉孢菌(*Neurospora crassa*)的 *Egt1* 基因和麦角菌(*Claviceps purpurea*)的 *Egt2* 基因用于构建 EGT 的生物合成途径。为解除前体供应不足所导致的代谢瓶颈，分别对组氨酸、半胱氨酸、甲硫氨酸及 *S*-腺苷甲硫氨酸的上游生物合成途径进行优化，以增强流向 EGT 合成的代谢通量。分别在摇瓶和 5 L 发酵罐中评价工程菌株的发酵性能。【结果】所构建的酿酒酵母工程菌株在摇瓶发酵条件下 EGT 产量为 312.8 mg/L。在 5 L 发酵罐中发酵 168 h 后 EGT 产量达 1 312.2 mg/L，生产强度为 7.8 mg/(L·h)。【结论】本研究提出了一种合成 EGT 的酿酒酵母代谢工程策略。该策略不仅显著提升了 EGT 的生物合成水平，也为其他化合物的微生物法生产提供了可借鉴的思路。

关键词：麦角硫因；酿酒酵母；代谢改造；前体供应；发酵优化

资助项目：国家重点研发计划(2022YFA0911800)；江苏省前沿技术研发计划(BF2025080)；中央引导地方科技发展资金(254Z2601G)
This work was supported by the National Key Research and Development Program of China (2022YFA0911800), the Frontier Technology Research and Development Plan of Jiangsu Province (BF2025080), and the Central Government Funds for Guiding Local Scientific and Technological Development (254Z2601G).
*Corresponding authors. E-mail: ZHAO Yunying, yunyingzhao@jiangnan.edu.cn; DENG Yu, dengyu@jiangnan.edu.cn
Received: 2026-02-13; Accepted: 2026-04-09; Published online: 2026-05-07

Metabolic engineering of *Saccharomyces cerevisiae* for the production of ergothioneine

Khan Salman, LI Xiaoxiao, YANG Qun, ZHAO Yunying*, DENG Yu*

Key Laboratory of Industrial Biotechnology of the Ministry of Education, School of Biotechnology, Jiangnan University, Wuxi, Jiangsu, China

Abstract: [Objective] Ergothioneine (EGT), a sulfur-rich derivative of histidine, is utilized in the food, pharmaceutical, and cosmetic industries. However, large-scale production of EGT faces challenges due to the high costs and inefficiency of conventional chemical synthesis and extraction techniques. This study aims to engineer *Saccharomyces cerevisiae* to provide a microbial platform for EGT biosynthesis. **[Methods]** The biosynthetic pathway for EGT was reconstructed in *S. cerevisiae* by heterologously expressing *Egt1* from *Neurospora crassa* and *Egt2* from *Claviceps purpurea*. To overcome the metabolic bottlenecks related to precursor supply, we optimized the upstream pathways for histidine, cysteine, methionine, and *S*-adenosylmethionine to enhance the flux toward EGT synthesis. Fermentation performance of the engineered strain was assessed in both shake flasks and a 5-L bioreactor. **[Results]** The engineered *S. cerevisiae* strain produced 312.8 mg/L of EGT in shake flask fermentation. In a 5-L bioreactor, the strain achieved the EGT titer of 1 312.2 mg/L after 168 h, with the productivity of 7.8 mg/(L·h). **[Conclusion]** This study presents a metabolic engineering strategy for producing EGT in *S. cerevisiae*. The approach not only significantly improves EGT biosynthesis but also serves as a reference for microbial production of other compounds.

Keywords: ergothioneine; *Saccharomyces cerevisiae*; metabolic engineering; precursor supply; fermentation optimization

Ergothioneine (EGT) is a unique sulfur-containing compound derived from histidine, produced from L-histidine and L-cysteine, with *S*-adenosyl-L-methionine (SAM) acting as the methyl donor in its biosynthesis[1]. The compound was initially discovered in the ergot fungus Claviceps purpurea in 1909[2]. Although EGT is commonly found in both plants and mammals[3], only specific microorganisms, such as certain bacteria and fungi—including *Cyanobacteria*, *Actinobacteria*, and *Basidiomycete* mushrooms have the ability to synthesize it[4-6]. In the solution, EGT interconverts between thiol and thione tautomers[7-8], with the thione form dominant under physiological conditions. This structural configuration underlies its remarkable resistance to autoxidation and contributes to its greater stability than that of classical thiol antioxidants such as glutathione[9-10]. Due to its robust redox buffering ability and protective effects on cells, EGT is gaining recognition as a bioactive metabolite with various physiological and therapeutic importance. Reported functions involve modulating inflammatory responses and reducing cellular aging processes[11-12], antidepressant-like effects, and protection from ultraviolet-induced oxidative stress[13-14].

In addition to its redox activity, EGT plays a vital role in cellular functions such as maintaining DNA synthesis, regulating cell growth, and

✉ actamicro@im.ac.cn, ☏ 010-64807516

supporting immune system health. It also offers radioprotective properties and is linked to skin-whitening and anti-aging effects, among various other physiological advantages[15]. Growing evidence suggests that EGT plays a significant role in chronic diseases, especially in neurodegenerative and cardiovascular conditions[16-17]. In a transgenic *Caenorhabditis elegans* model of Alzheimer's disease that expresses human β-amyloid, supplementing with EGT improved both healthspan and lifespan[18]. In humans, circulating EGT levels have been identified as a strong biomarker linked to a decreased risk of cardiovascular disease and lower all-cause mortality in a Swedish population cohort study[19]. Due to its antioxidant and cytoprotective properties, EGT has gained significant interest for use in medical and cosmetic applications. However, low yields from plant-based extraction restrict the scalability of EGT production[20]. The chemical synthesis of EGT is challenging because of its chiral amino acid structure, making downstream separation and purification more complicated[21]. As a result, metabolic engineering and microbial fermentation have emerged as primary research areas to boost EGT production, given their advantages of higher yields, lower costs, and greater sustainability[22].

The biosynthesis pathway of EGT varies considerably among microorganisms, especially between bacteria and fungi. Bacterial species produce EGT through a five-enzyme process, from *EgtA* to *EgtE*. In *Mycobacterium smegmatis*, the pathway involves histidine, cysteine, glutamate, and methionine, ultimately leading to the formation of EGT[23]. In contrast, fungi like *Neurospora crassa* use a simpler two-enzyme pathway (Figure 1) involving *Egt1* and *Egt2*[24]. In the bacterial pathway, L-histidine initially undergoes methylation by the SAM-dependent methyltransferase *EgtD*, resulting in the formation of hercynine (HER)[25]. The mononuclear non-heme iron enzyme *EgtB* then catalyzes the transformation of hercynine into γ-glutamyl-hercynylcysteine sulfoxide (γGC-HER), using γ-glutamylcysteine produced by *EgtA* as the sulfur donor[26]. The amidohydrolase *EgtC* then cleaves the glutamate part, forming hercynylcysteine sulfoxide (Cys-HER), which is subsequently transformed into EGT through the action of the pyridoxal-5′-phosphate (PLP)-dependent β-lyase *EgtE*[27]. In the *N. crassa* fungal pathway, the multifunctional enzyme *Egt1* methylates L-histidine to produce hercynine and also catalyzes its conversion to hercynylcysteine sulfoxide[28]. The second step enzyme, *Egt2*, acts similarly to bacterial *EgtE* by cleaving the C−S bond of hercynylcysteine sulfoxide through a PLP-dependent cysteine desulfurase reaction to produce EGT[29-30].

To date, various organisms have been genetically modified to produce EGT. Osawa et al. initially overexpressed the five enzymes from *M. smegmatis*: *EgtA*, *EgtB*, *EgtC*, *EgtD*, and *EgtE*[31]. Supplements of thiosulfate, which provide sulfur for cysteine, boosted γ-glutamylcysteine production, leading to a 120-fold rise in EGT yield from 0.2 to 24 mg/L after optimizing fermentation conditions. Similarly, the *N. crassa Egt1* and *Egt2* genes were inserted into the *Aspergillus oryzae* genome in multiple copies, resulting in an EGT production of 231 mg/kg on solid media[32]. Another study showed that *S. cerevisiae* can be genetically engineered to produce significant amounts of EGT, reaching 598 mg/L in a fed-batch bioreactor process[33]. However, the expression of the *Gfegt1* and *Gfegt2* genes from *Grifola frondosa* in the engineered *S. cerevisiae* strain resulted in an EGT titer of only 20.61 mg/L[34]. Interestingly, recombinant *S. cerevisiae* was engineered to express *Aspergillus fumigatus* methyltransferase and sulfoxide synthase (*egtA*), which produced just 7.93 mg/L of EGT in shake-flask culture. Because *S. cerevisiae* does not naturally have EGT biosynthetic genes, the detected EGT formation through C−S bond cleavage, which is normally facilitated by *Egt2* or *EgtE*, may be caused by the yeast's own enzymes or abiotic chemical reactions[35]. An alternative approach involved

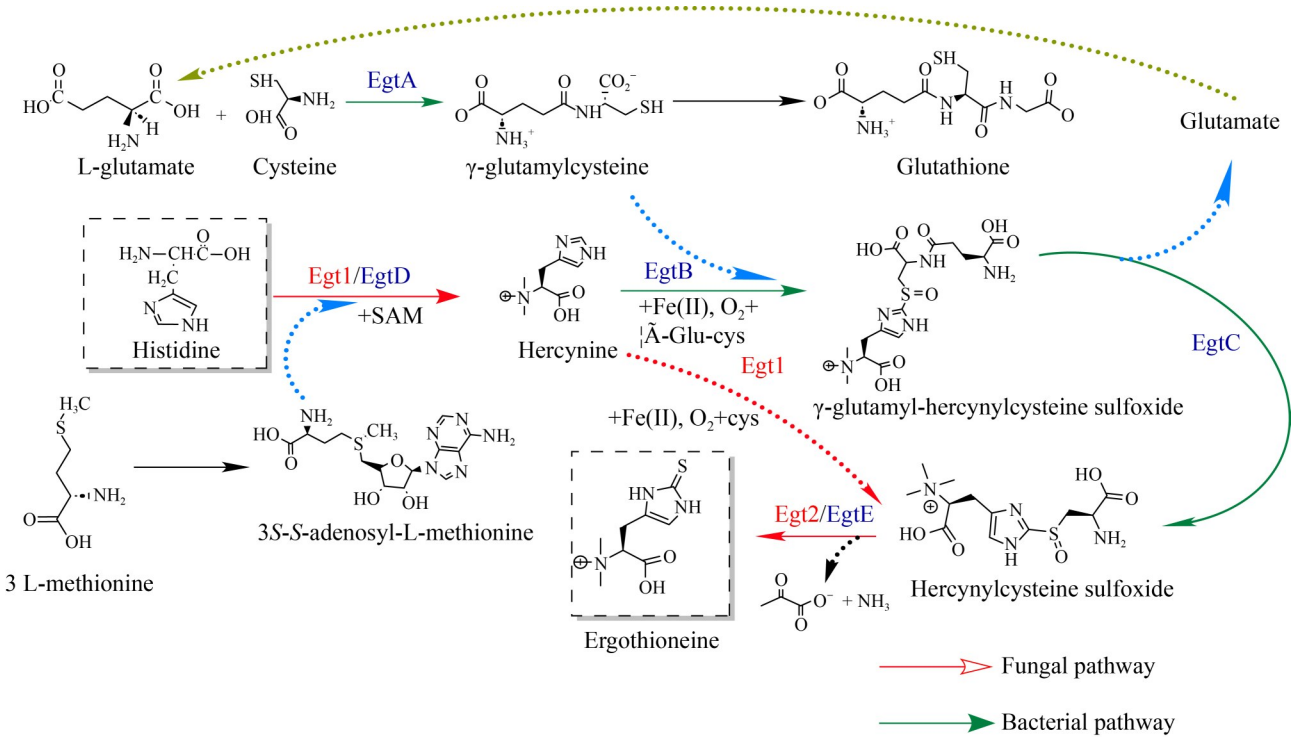

Figure 1 Biosynthetic pathways of EGT in both prokaryotic and eukaryotic systems. Enzymes highlighted in blue are those found in prokaryotes. EgtA: γ-glutamylcysteine synthetase; EgtB: Non-heme iron-dependent mononuclear oxidase; EgtC: Amidotransferase; EgtD: *S*-adenosylmethionine-dependent histidine methyltransferase; EgtE: PLP-dependent C−S lyase. Enzymes depicted in red indicate their eukaryotic counterparts; Egt1: A bifunctional enzyme with SAM-dependent histidine methyltransferase and non-heme iron-dependent oxidase activities; Egt2: A PLP-dependent C−S lyase. The light blue dashed lines denote amino acids that serve as essential precursors.

adding an extra native *egtBD* copy and deleting the histidine ammonia-lyase gene *hutH* in *Methylobacterium aquaticum*, resulting in a strain that produced 7.0 mg/g (dry cell weight, DCW) of EGT over seven days[36]. Likewise, introducing the *egtB* gene from *M. pseudosasicola* into a cysteine- and methionine-overproducing *E. coli* strain led to the production of 657 mg/L EGT after 192 hours of cultivation with added histidine and methionine. However, fed-batch fermentation was not feasible due to the slow growth of the strain[37]. Meanwhile, an *E. coli* strain was engineered to enhance cysteine production by activating its synthesis and secretion pathways. This involved heterologous expression of *M. smegmatis egtA*, *egtB*, *egtC*, *egtD*, and *egtE*, along with knocking out the methionine repressor gene *metJ*. After 216 hours of fed-batch fermentation in a 3-L bioreactor, a yield of 1.3 g/L EGT was achieved[38]. In *E. coli*, boosting the SAM cycle and rebuilding the EGT biosynthesis pathway resulted in about 2.52 g/L of EGT in fed-batch culture, due to increased precursor and cofactor supplies[39]. Expression of *Trichoderma reesei Tregt1* and *Tregt2* in *E. coli via* whole-cell catalysis and fed-batch fermentation produced 4.34 g/L of extracellular EGT after 143 hours in a 2-L bioreactor[40].

Introducing *N. crassa egt1* and *M. smegmatis egtD* and *egtE* into *E. coli*, along with mutagenesis of *egt1* and *egtD* and fermentation optimization,

led to an EGT production of 5.4 g/L[41]. By employing a multicopy genomic integration approach in *Yarrowia lipolytica*, the researchers achieved an ergothioneine production level of 7.3 g/L in fed-batch fermentation[42]. By combining enzyme engineering (*Tregt1* mutations) in *Y. lipolytica*, systematic enhancement of the precursor pathway, and optimized fermentation conditions, production reached 9.3 g/L EGT in a 5-L bioreactor after 168 hours, with a productivity of 55.35 mg/(L·h)[43].

Although many metabolic engineering projects focus on prokaryotic hosts, *S. cerevisiae* has significant advantages as a Generally Recognized as Safe (GRAS) organism widely used in the food and nutraceutical industries. It provides high regulatory approval, reduced endotoxin risk, and easier downstream processing. Its eukaryotic architecture ensures correct folding of heterologous enzymes, while strong sulfur and amino acid metabolic pathways, including those for histidine, cysteine, methionine, and SAM, provide essential precursors for EGT production. Furthermore, yeast demonstrates significant stress tolerance and the ability to reach high cell densities in aerobic environments. This study presents a systematic metabolic engineering strategy to boost EGT production in *S. cerevisiae* by concurrently optimizing precursor supply, methyl donor availability, and enzyme capacity within the pathway. The precursor metabolic network was modularly engineered to enhance sulfur assimilation and the production of methionine, histidine, and cysteine. We particularly reinforced the methionine-SAM axis to raise intracellular SAM levels and reduced competing pathways that use SAM. Moreover, ATP-producing genes were upregulated to support the higher biosynthetic demand, and multiple copies of *Egt1* and *Egt2* were integrated to boost pathway capacity. This work develops a comprehensive metabolic engineering framework by coordinating improvements in precursor metabolism, methyl donor supply, and enzymatic steps, offering new insights into increasing EGT production in yeast.

1 Materials and methods

1.1 Strains and media

The *S. cerevisiae* strain CEN.PK2, maintained in our laboratory, was used as the parental strain for all genetic modifications, whereas *E. coli* JM109 was used for plasmid construction and amplification (Table 1). *E. coli* cultures were grown in lysogeny broth (LB) and on LB agar containing 100 mg/L ampicillin at 37 ℃. Yeast cells were cultured in yeast extract-peptone-dextrose (YPD) medium, made with 20 g/L glucose, 20 g/L peptone, and 10 g/L yeast extract, at 30 ℃ with shaking at 200 r/min. For the Cas9 vector selection, we supplemented YPD media with G418 and maintained its concentration at 200 mg/L. For the gRNA vector, 100 mg/L hygromycin (HYG) was added to YPD media. To apply selective pressure, the yeast strains were grown in SD medium (6.7 g/L yeast nitrogen base without amino acids, 2% glucose) supplemented with the appropriate amino acids. The plasmid pRS423 contains the HIS3 marker, while the pHAC181 plasmid carries the LEU2 marker. Accordingly, the amino acids were supplemented in the SD medium during the transformation of the plasmids in the yeast strains. Minimal medium (MM) was formulated for controlled yeast cultivation, consisting of 7.5 g/L $(NH_4)_2SO_4$, 14.4 g/L KH_2PO_4, 0.5 g/L $MgSO_4·7H_2O$, 2 mL/L trace metal solution, and 1 mL/L vitamin solution. The trace metal solution contained 4.5 g/L $CaCl_2·2H_2O$, 4.5 g/L $ZnSO_4·7H_2O$, 3 g/L $FeSO_4·7H_2O$, 1 g/L H_3BO_3, 1 g/L $MnCl_2·4H_2O$, 0.4 g/L $Na_2MoO_4·2H_2O$, 0.3 g/L $CoCl_2·6H_2O$, 0.1 g/L $CuSO_4·5H_2O$, 0.1 g/L KI, and 15 g/L EDTA. The vitamin solution comprised 50 mg/L biotin, 200 mg/L p-aminobenzoic acid, 1 g/L nicotinic acid, 1 g/L pyridoxine HCl, 1 g/L thiamine HCl, and 25 g/L *myo*-inositol. All media components were sterilized by autoclaving at 121 ℃ for 20 min or by filtration when heat-sensitive. Cultures were initiated under sterile conditions to ensure reproducibility, optimal

Table 1 Strains used in this study

Strain name	Genotype/Modifications	Construction details	Sources
CEN-PK2	CEN.PK113-7D Mata MAL2-8c SUC2 URA3 HIS3 LEU2 TRP1	Parent strain	Lab store
JM109	Wild type, for plasmid construction		Lab store
ST4001	CEN-PK2 expressing pRS423-*Tregt1* and pHAC181-*Cpegt2*	Overexpressing *Tregt1* and *Cpegt2* in CEN-PK2	This study
ST4002	CEN-PK2 expressing pRS423-*Tregt1* and pHAC181-*Rtegt2*	Overexpressing *Tregt1* and *Rtegt2* in CEN-PK2	This study
ST4003	CEN-PK2 expressing pRS423-*Tregt1* and pHAC181-*Spegt2*	Overexpressing *Tregt1* and S*pegt2* in CEN-PK2	This study
ST4004	CEN-PK2 expressing pRS423-*Tregt1* and pHAC181-*MsegtE*	Overexpressing *Tregt1* and *MsegtE* in CEN-PK2	This study
ST4005	CEN-PK2 expressing pRS423-*Tregt1* and pHAC181-*Tregt2*	Overexpressing *Tregt1* and Tr*egt2* in CEN-PK2	This study
ST4006	CEN-PK2 expressing pRS423-*Ncegt1* and pHAC181-*Cpegt2*	Overexpressing *Ncegt1* and *Cpegt2* in CEN-PK2	This study
ST4007	CEN-PK2 expressing pRS423-*Rtegt1* and pHAC181-*Cpegt2*	Overexpressing *Rtegt1* and *Cpegt2* in CEN-PK2	This study
ST4008	CEN-PK2 expressing pRS423-*Spegt1* and pHAC181-*Cpegt2*	Overexpressing *Spegt1* and *Cpegt2* in CEN-PK2	This study
ST4009	ST4006 Δ*HO*::P_{TDH3}-*SAM2*-T_{CYC1}	Overexpressing *SAM2* in T4006	This study
ST4010	ST4009 Δ*GAL80*::P_{TDH3}-*CYS3*-T_{CYC1}	Overexpressing *CYS3* in T4009	This study
ST4011	ST4010 Δ*YGR250*::P_{TDH3}-*HIS1*-T_{CYC1}	Overexpressing *HIS1* in T4010	This study
ST4012	ST4010 Δ*DIT1*::P_{TDH3}-STR2-T_{CYC1}	Overexpressing *STR2* in T4010	This study
ST4013	ST4012 *NDT80*::P_{TEF1}-*MET6*-T_{CYC1}	Overexpressing *MET6* in T4012	This study
ST4014	ST4011 Δ*DIT1*::P_{TDH3}-*STR2*-T_{CYC1}	Overexpressing *STR2* in T4011	This study
ST4015	ST4014 *NDT80*::P_{TEF1}-*MET6*-T_{CYC1}	Overexpressing *MET6* in T4014	This study
ST4016	ST4015 *GAL2*::P_{TEF1}-*ADK1*-T_{CYC1}	Overexpressing *ADK1* in T4015	This study
ST4017	ST4016 P_{HXT1}-*ERG6*-T_{CYC1}	Downregulation of the *ERG6* gene in ST4016	This study
ST4018	ST4017 P_{HXT1}-*ERG4*-T_{CYC1}	Downregulation of the *ERG4* gene in ST4017	This study
ST4019	ST4018 P_{HXT1}-*SPE2*-T_{CYC1}	Downregulation of the *SPE2* gene in ST4018	This study
ST4020	ST4019 rDNA::P_{TDH3}-*Ncegt1*-T_{CYC1}	Multicopy integration of *Ncegt1* in ST4019	This study
ST4021	ST4020 delta::P_{TDH3}-*Cpegt2*-T_{CYC1}	Multicopy integration of *Cpegt2* in ST4020	This study
ST4022	CEN-PK2 Δ*GAL80*::T_{CYC1}-*Ncegt1*-P_{TDH3}-P_{TDH3}-*Cpegt2*-T_{CYC1}	Single copy integration of *Ncegt1* and *Cpegt2* in CEN-PK2	This study

growth, and suitability for downstream genetic and fermentation experiments.

1.2 Construction of plasmids and strains

For the production of *EGT*, the genes *Egt1* and *Egt*2 were obtained from various organisms known for their EGT biosynthesis. These genes, along with their respective accession numbers, are as follows: *Egt1* from *N. crassa* (accession No. XP_956324.3, *Ncegt1*), *Egt2* from *C. purpurea* (accession No. CCE33140.1, *Cpegt2*), *Egt1* from *Schizosaccharomyces pombe* (accession No. NP_596639.2, *Spegt1*), *Egt2* from *S. pombe*

(accession No. NP_595091.1, *Spegt2*), *EgtE* from *M. smegmatis* (accession No. ABK70212.1, *MsegtE*), *Egt1* from *Trichoderma reesei* (accession No. XP_006968620, *Tregt1*), *Egt2* from *T. reesei* (accession No. XP_006968735, *Tregt2*), and *Egt1* from *Rhodotorula toruloides* (accession No. XP_016270018.1, *Rtegt1*), *Egt2* from *Rhodotorula toruloides* (accession No. XP_016270654.1, *Rtegt2*). These genes were codon-optimized for *S. cerevisiae* to ensure high expression efficiency in the yeast host. Codon optimization was performed by Azenta Life Sciences (Suzhou, China).

The plasmids used in this study are listed in Table 2. The P_{TDH3} and P_{TEF1} promoter, along with the T_{CYC1} and T_{ADH1} terminator, were amplified from the BY4741 genome. The gene fragments of *Egt1* and *Egt2* were amplified directly from the synthesized DNA using high-fidelity Phusion DNA polymerase (Vazyme, Nanjing, China). These gene fragments were then fused in a series of PCR reactions, in which two gene fragments (P_{TDH3}-Egt1-T_{CYC1} and P_{TEF1}-Egt2-T_{ADH1}) were joined to ensure proper gene expression and termination in yeast. The sequences of the *Egt1* cassette were cloned into the pRS423 plasmid, and the sequences of the *Egt2* cassette were cloned into the pHAC181 plasmid. The plasmids were assembled using the Gibson Assembly system, and Sanger sequencing verified the integrity of the constructs.

For genome editing in *S. cerevisiae*, we used two plasmids provided by our lab: pRS42H-gRNA, a plasmid for expressing the CRISPR guide RNA to generate sgRNAs, and p414-P_{TEF1}-Cas9-T_{CYC1}-KanMX, a plasmid for expressing the Cas9 nuclease. These plasmids were used together to enable precise genome modifications in *S. cerevisiae* by integrating the desired genes *via* a CRISPR-Cas9-based genome editing approach. To facilitate genome editing, single-guide RNAs (sgRNAs) were designed using the CHOPCHOP tool (https://chopchop.cbu.uib.no/) to target specific genomic loci for gene integration and deletion. The sgRNAs were cloned into a plasmid vector designed to insert into a Cas9-expressing cassette.

Table 2 Plasmids used in this study

Plasmids	Description	Sources
pRS423	High-copy 2μ yeast expression plasmid	Lab store
p HAC181	High-copy 2μ yeast expression plasmid	Lab store
pRS423-*Ncegt1*	pRS423 plasmid carrying *Ncegt1*	This study
pRS423-*Rtegt1*	pRS423 plasmid carrying *Rtegt1*	This study
pRS423-*Spegt1*	pRS423 plasmid carrying *Spegt1*	This study
pRS423-*Tregt1*	pRS423 plasmid carrying *Tregt1*	This study
pHAC181-*Cpegt2*	pHAC181 plasmid carrying *Cpegt2*	This study
pHAC181-*MsegtE*	pHAC181 plasmid carrying *MsegtE*	This study
pHAC181-*Rtegt2*	pHAC181 plasmid carrying *Rtegt2*	This study
pHAC181-*Spegt2*	pHAC181 plasmid carrying *Spegt2*	This study
pHAC181-*Tregt2*	pHAC181 plasmid carrying *Tregt2*	This study
pRS42H_gRNA-GAL2	CRISPR guide RNA expression plasmid	This study
pRS42H_gRNA-GAL80	CRISPR guide RNA expression plasmid	This study
pRS42H_gRNA-YGR250	CRISPR guide RNA expression plasmid	This study
pRS42H_gRNA-NDT80	CRISPR guide RNA expression plasmid	This study
pRS42H_gRNA-HO	CRISPR guide RNA expression plasmid	This study
pRS42H_gRNA-DIT1	CRISPR guide RNA expression plasmid	This study
p414-P_{TEF1}-Cas9-T_{CYC1}	Cas9 expression plasmid	Lab store

These plasmids were then introduced into yeast cells to achieve precise genome modifications.

1.3 qPCR analysis

Firstly, the total RNA from the ST4021, ST4016, and ST4022 strains was isolated by using Ultrapure RNA Kit (CWBIO, Beijing) following the manufacturer's instructions. Then, the first-strand cDNA synthesis was subsequently performed using the HIScriptIV 1st Strand cDNA Synthesis Kit (Vazyme, Nanjing) according to the manufacturer's instructions. Quantitative real-time PCR (qPCR) was conducted on a CFX96 Real-Time Thermal Cycler (Step OnePlus, American Applied Biosystems Corporation) using the *Taq* Pro Universal qPCR Master Mixture (Vazyme, Nanjing). Relative gene expression levels were calculated employing the $2^{-\Delta\Delta C_t}$ method, with the housekeeping gene *PGK1* serving as the endogenous reference for normalization. The final data are presented as the mean relative fold change in expression compared to the control strain ST4022.

1.4 Shake flask fermentation

Strains preserved in glycerol stocks were first streaked onto SD agar plates and incubated at 30 ℃ for 2 − 3 days to obtain single colonies. A well-isolated colony was inoculated into a 50 mL shake tube containing 5 mL of sterilized YPD medium and cultured at 30 ℃ with shaking at 220 r/min for 14 to 16 hours to produce an actively growing pre-culture. To ensure consistent inoculation and strong growth, 5% (*V*/*V*) of this pre-culture was transferred into a 250 mL shake flask containing 50 mL of YPD medium (1:5 flask-to-medium volume ratio for optimal aeration) and incubated at 30 ℃ with shaking at 220 r/min for up to 120 hours. During cultivation, samples were periodically taken to monitor optical density at 600 (OD_{600}). Culture supernatants were clarified *via* centrifugation and analyzed for EGT content with high-performance liquid chromatography (HPLC), ensuring precise measurement of metabolite production during the fermentation process.

To determine the optimal production conditions for EGT, the concentrations of L-methionine (Met), L-histidine (His), L-cysteine (Cys), and L-arginine (Arg) were varied across six experimental groups (A to F). Group A: 1 g/L Met, His, Cys, and Arg were added to the culture medium. Group B: 5 g/L of Met, 5 g/L of His, and 5 g/L of Cys and Arg were added to the culture medium. Group C: 10 g/L of Met, 4 g/L of His, and 10 g/L of Cys and Arg were added to the culture media. Group D: 20 g/L of Met, 8 g/L His, and 8 g/L Cys and Arg were added to the culture medium. Group E: 25 g/L Met, 12 g/L His, 12 g/L Cys, and Arg were added to the culture medium. Group F: 30 g/L Met, 16 g/L His, and 16 g/L Cys and Arg were added to the culture medium.

1.5 Fed-Batch fermentation

Glycerol stock strains were streaked on SD agar plates to isolate colonies. Ten well-isolated colonies were individually selected and inoculated into 50 mL shake flasks with 10 mL SD medium. These were incubated at 30 ℃ with orbital shaking at 220 r/min for 24 hours to generate seed cultures. Next, 5% (*V*/*V*) of each seed culture was transferred into 250 mL shake flasks containing 100 mL SD medium, then incubated at the same temperature and shaking speed for another 24 hours.

For large-scale production, a 5% (*V*/*V*) inoculum was added to a 5-L bioreactor containing 2.5 L of YPD medium with 20 g/L yeast extract, 40 g/L peptone, and an initial glucose concentration of 50 g/L. To increase the EGT precursor availability, L-methionine (20 g/L), L-histidine (8 g/L), L-cysteine (8 g/L), and L-arginine (8 g/L) were added directly to the fermentation medium before sterilization as a single initial supplement. The bioreactor was maintained at 30 ℃ with a maximum agitation speed of 500 r/min to ensure proper mixing and oxygen transfer. Dissolved oxygen was rigorously controlled at 20%, and pH was stabilized near 5.0 through automated addition of pure ammonia. At 24 hours, 0.05 g/L of butylated hydroxytoluene was added as an antioxidant. Additionally, an antifoam agent was

added to reduce foam formation during fermentation and ensure a smooth, efficient process.

Glucose consumption was closely monitored throughout the fermentation using a controlled feeding strategy. A sterile glucose stock solution (450 g/L) served as the feed. Glucose was supplemented *via* pulse feeding at approximately 10 g/L every 24 hours. Samples were collected at defined intervals to determine optical density, residual glucose concentration, and EGT production.

1.6 Compound analysis

After the fermentation process, extracellular EGT was measured by taking 1 mL of fermentation broth, which was then immediately centrifuged at 3 000×*g* for 5 minutes at 4 ℃ to preserve metabolite stability. The clear supernatant was subsequently transferred to HPLC vials for analysis using high-performance liquid chromatography (HPLC). To measure intracellular EGT, the remaining cell pellet was washed twice with 1 mL of Milli-Q water and then resuspended in 1 mL of water. The extraction of intracellular EGT was carried out as described by Alamgir et al. (2015)[44]. For yeast cell optimization, the suspension was heated at 94 ℃ for 10 minutes, vortexed at 1 600 r/min for 30 minutes, and centrifuged at 10 000×*g* for 5 minutes. The supernatant was then collected into HPLC vials for analysis. All samples were filtered through 0.22 μm membranes immediately prior to injection to remove residual particulates.

EGT quantification was conducted using HPLC with a mobile phase of methanol and ultrapure water in a 1:99 ratio. Chromatography was performed at 30 ℃ , with a flow rate of 1 mL/min, an injection volume of 10 μL, and UV detection at 257 nm. Each run lasted 18 min, providing accurate and reproducible measurements of both extracellular and intracellular EGT. All tests were performed in triplicate, and system suitability was verified with standard EGT solutions before analyzing samples to ensure consistency and precision.

2 Results and analysis

2.1 Construction and optimization of the ergothioneine biosynthetic pathway in *S. cerevisiae*

To establish an effective EGT biosynthesis pathway in *S. cerevisiae*, we first evaluated the functional diversity of EGT-synthetase homologs from fungal and bacterial origins. A panel of *Egt1* and *Egt2* genes was chosen based on their phylogenetic diversity and previous reports of EGT production, including homologs from fungi *N. crassa* (*Ncegt1*), *R. toruloides* (*Rtegt1* and *Rtegt2*), *S. pombe* (*Spegt1* and *Spegt2*), *T. reesei* (*Tregt1* and *Tregt2*), and *C. purpurea* (*Cpegt2*), as well as the bacterial *EgtE* gene from *M. smegmatis* (*MsegtE*). Each *Egt1* homolog was paired separately with its corresponding *Egt2* gene to evaluate the combined pathway efficiency in yeast for EGT production (Figure 2). Eight different EGT-producing strains were developed in *S. cerevisiae* to study how enzyme origin and pathway setup affect EGT production. Seven strains contained only fungal genes, whereas one hybrid strain combined fungal and bacterial homologs. These strains were grown under controlled conditions, and measurements were taken of both intracellular and extracellular EGT levels.

Among these eight strains, five shared *Egt1* from *T. reesei*, each paired with diverse second-step enzymes (*Cpegt2*, *MsegtE*, *Rtegt2*, *Spegt2*, and *Tregt2*). Within this group, strain ST4001 reached a titer of 22.0 mg/L extracellularly and 17.0 mg/L extracellularly with total accumulation of 39.0 mg/L, reflecting moderate pathway efficiency (Figure 2A). Therefore, the remaining three strains all contained *Cpegt2* from *C. purpurea* as the common second-step enzyme, combined with alternative first-step enzymes (*Ncegt1*, *Rtegt1*, and *Spegt1*). Notably, strain ST4006, carrying the *Ncegt1* and *Cpegt2* combination, achieved the highest EGT titer of 36.0 mg/L extracellular and 20.0 mg/L intracellularly with a total of 56.0 mg/L

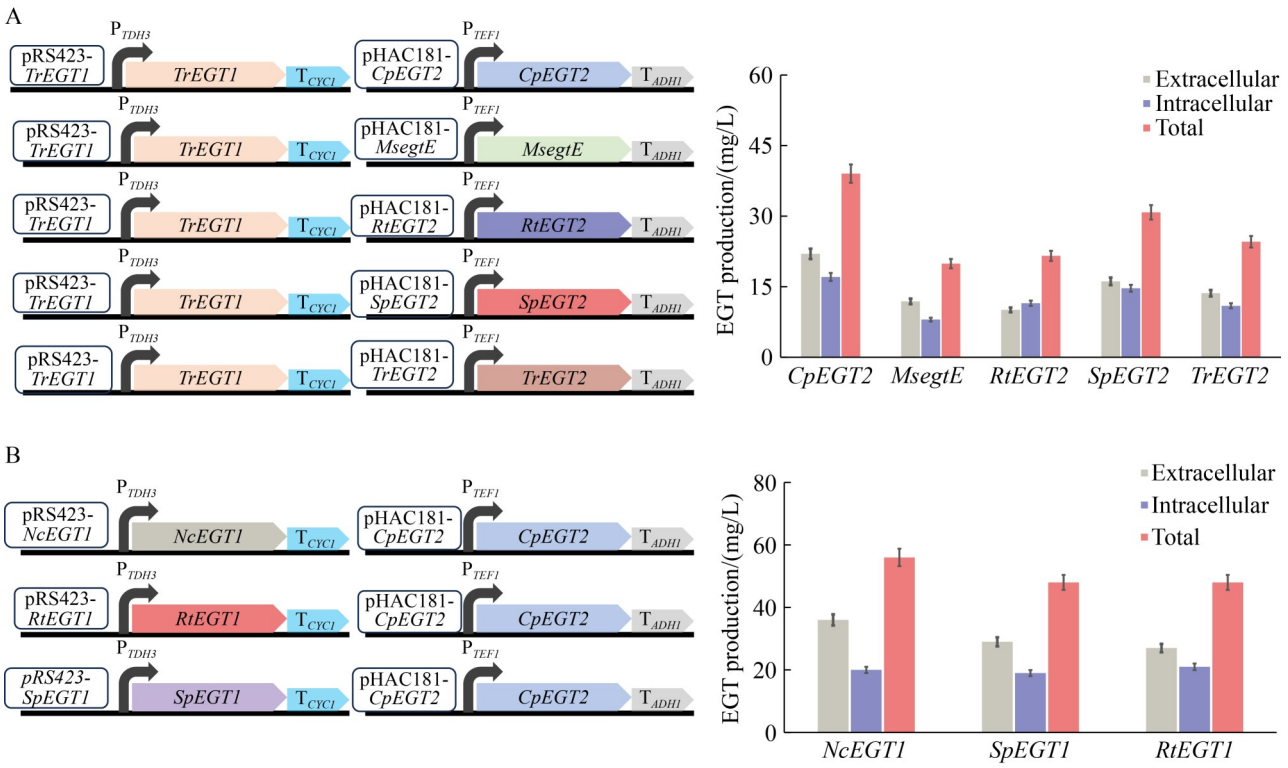

Figure 2 Construction of the EGT synthesis pathway in *Saccharomyces cerevisiae*. A: Evaluation of *Tregt1* and five *Egt2* variants in EGT production; B: Evaluation of *Cpegt2* and three *Egt1* variants in EGT biosynthesis.

(Figure 2B), highlighting the critical impact of enzyme selection on pathway performance. ST4006, combining *N. crassa Egt1* and *C. purpurea Egt2*, was selected for further engineering.

2.2 Reinforcing precursor amino acid biosynthesis boosts ergothioneine production

S-adenosyl-L-methionine is essential for EGT biosynthesis because it provides the methyl groups required for the three methylation steps carried out by *Egt1*. Thus, the level of SAM inside the cell directly influences the activity of the pathway. In *S. cerevisiae*, native methylation processes such as those involved in phospholipid, histone, and polyamine synthesis consume SAM, further limiting EGT production[45]. Among the two SAM synthetases in yeast, the one that is more responsive to metabolic demand and more effectively increases SAM pools when engineered is the preferred target[46]. SAM2, encoding SAM synthase, was overexpressed in strain ST4009 to boost EGT accumulation (Figure 3A and 3B). The results demonstrated that overexpressing the SAM2 gene led to increased EGT production, reaching 50.6 mg/L extracellularly and 31.1 mg/L intracellularly, with a total of 81.7 mg/L. This indicates that SAM2 enhances EGT synthesis (Figure 3B).

Histidine and cysteine are crucial precursors for EGT biosynthesis, where histidine offers the imidazole scaffold and cysteine provides the sulfur atom necessary for thiol or thione formation[47]. However, intracellular histidine levels remain a significant limitation because His1, the first committed enzyme in the pathway, is strongly inhibited by histidine itself[48]. To overcome these precursor bottlenecks, we systematically enhanced the supply of both sulfur and imidazole precursors. First, *CYS3* was overexpressed in strain ST4009 to generate strain ST4010, thereby increasing cysteine

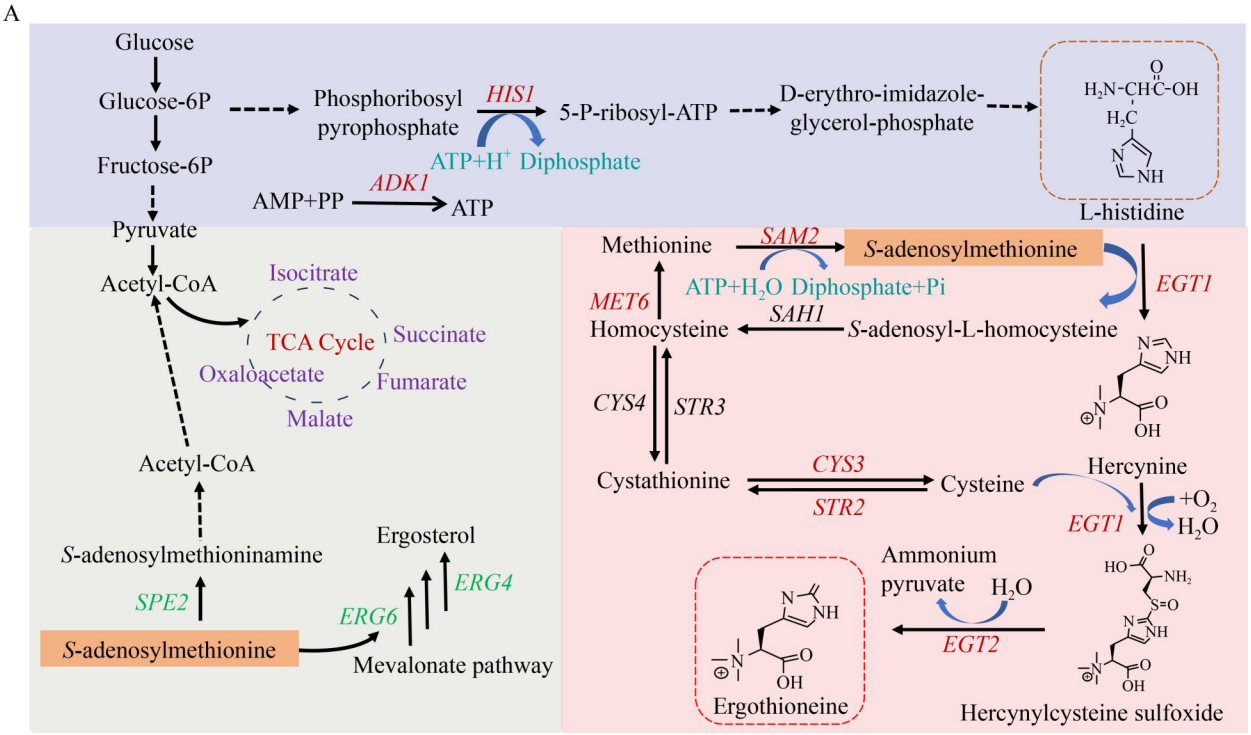
A
Glucose
Glucose-6P
Fructose-6P
Pyruvate
Acetyl-CoA
Isocitrate
TCA Cycle
Succinate
Oxaloacetate
Fumarate
Malate
Acetyl-CoA
S-adenosylmethioninamine
SPE2
S-adenosylmethionine
Phosphoribosyl pyrophosphate
HIS1
5-P-ribosyl-ATP
ATP+H+ Diphosphate
D-erythro-imidazole-glycerol-phosphate
L-histidine
ADK1
AMP+PP
ATP
Ergosterol
ERG4
ERG6
Mevalonate pathway
Methionine
SAM2
S-adenosylmethionine
ATP+H2O Diphosphate+Pi
EGT1
MET6
SAH1
Homocysteine
S-adenosyl-L-homocysteine
CYS4
STR3
Cystathionine
CYS3
STR2
Cysteine
Hercynine
+O2
H2O
EGT1
Ammonium pyruvate
H2O
EGT2
Ergothioneine
Hercynylcysteine sulfoxide

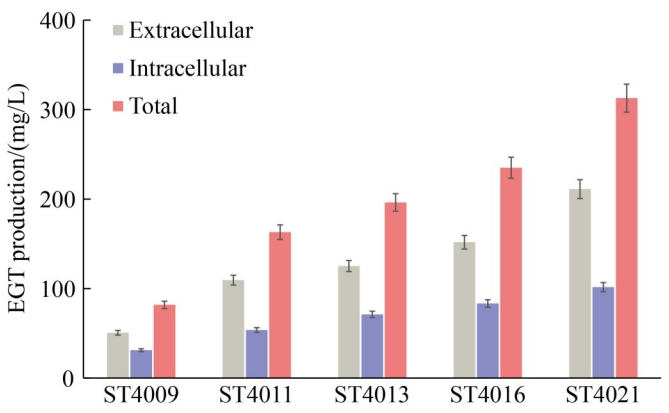
B
EGT production/(mg/L)
Extracellular
Intracellular
Total
ST4009
ST4011
ST4013
ST4016
ST4021

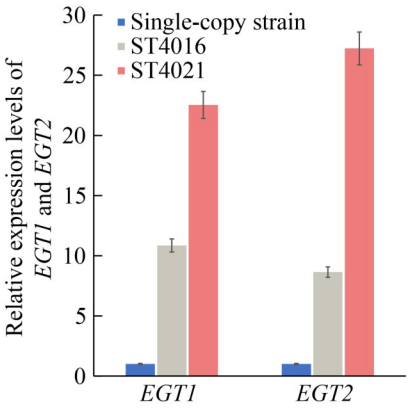
C
Relative expression levels of EGT1 and EGT2
Single-copy strain
ST4016
ST4021
EGT1
EGT2

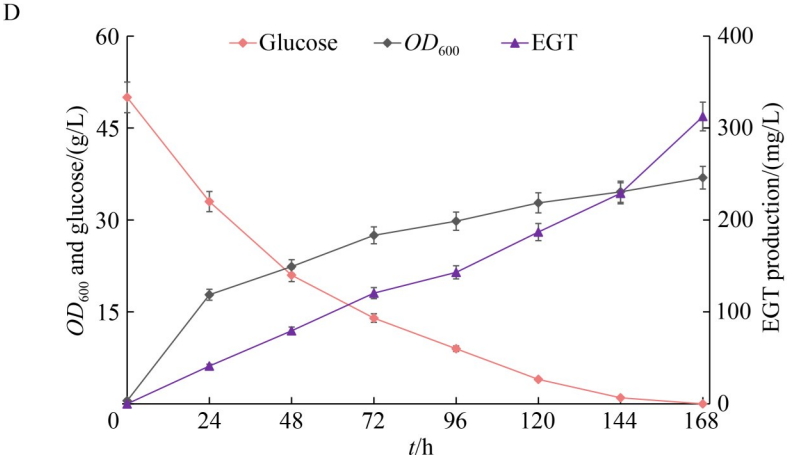
D
Glucose
OD600
EGT
OD600 and glucose/(g/L)
EGT production/(mg/L)
t/h

Figure 3 Metabolic engineering to improve the supply of essential amino acid precursors. A: Schematic overview of the engineered metabolic strategies; B: Metabolic engineering of key genes in the EGT pathway to increase its titer. *SAM2* gene was overexpressed in strain ST4009, three genes of *SAM2*, *CYS3*, and *HIS1* were overexpressed in strain ST4011, three genes of *SAM2*, *STR2*, and *MET6* were overexpressed in strain ST4013, six genes of *SAM2*, *CYS3*, *HIS1 STR2*, *MET6*, and *ADK1* were overexpressed in strain ST4016, six genes of *SAM2*, *CYS3*, *HIS1*, *STR2*, *MET6*, and *ADK1* were overexpressed and three genes of *ERG6*, *ERG4*, and *SPE2* were downregulated in strain ST4021, and *Ncegt1* and *Cpegt2* were integrated with multiple copies; C: Relative expression levels of *Egt1* and *Egt2* in ST4016 and ST4021 compared to the single-copy strain; D: The flask fermentation process of strain ST4021.

availability for sulfur incorporation. Building on this, we enhanced histidine biosynthesis by co-expressing *HIS1* under the strong constitutive *TDH3* promoter, resulting in the creation of the ST4011 strain. Overexpression of *SAM2*, *CYS3*, and *HIS1* led to a significant, synergistic increase in EGT production, with no apparent effect on cell growth. Strain ST4011 was found to produce 109.4 mg/L extracellular and 53.6 mg/L intracellular with a total of 163.0 mg/L EGT (Figure 3B). Compared to strain ST4009, the extracellular EGT increased by 116.3%, and the intracellular levels increased by 72.0%, respectively. The results demonstrate that simultaneously increasing histidine and cysteine supply effectively alleviates key metabolic bottlenecks in EGT biosynthesis.

Increasing L-methionine supply, the immediate precursor of SAM, can effectively boost SAM production *via* bacterial fermentation[47]. Therefore, our goal was to improve the expression of other crucial genes in the SAM biosynthesis pathway, such as *MET6* and *STR2*, to raise intracellular SAM levels and thereby enhance EGT production (Figure 3A). The *STR2* gene was overexpressed in strain ST4009 to generate ST4012. Subsequently, the *MET6* gene was overexpressed in ST4012, yielding the new strain of ST4013, in which all target genes, *SAM2*, *STR2*, and *MET6*, were simultaneously overexpressed. Strain ST4013 produced 125.1 mg/L extracellular and 71.1 mg/L intracellular with a total of 196.2 mg/L of EGT. Compared with strain ST4011, extracellular EGT increased by 14.4%, while intracellular levels increased 32.6%. To further reinforce precursor and cofactor supply, we expanded the engineering strategy used in ST4011, which already overexpressed *SAM2*, *CYS3*, and *HIS1*. In ST4016, we additionally integrated the *STR2* and *MET6* expression cassettes at the same genomic locus used in strain ST4013, thereby enhancing methionine and SAM biosynthesis. Furthermore, *ADK1* was overexpressed to improve adenylate balance and facilitate efficient ATP regeneration, thereby further strengthening SAM formation. Flask fermentation of the resulting strain ST4016 showed a substantial increase in EGT production. Strain ST4016 accumulated 151.8 mg/L extracellular and 83.3 mg/L intracellular with a total of 235.1 mg/L of EGT. Compared with strain ST4013, extracellular and intracellular levels increased by 21.3% and 17.1%, respectively. These results demonstrate that simultaneously increasing histidine, cysteine, methionine, and SAM, along with improved ATP regeneration, leads to a synergistic improvement in overall EGT flux (Figure 3B).

2.3 Enhancing SAM availability by downregulating SAM-consuming pathways and increasing the expression of *Egt1* and *Egt2*

SAM serves as the primary methyl donor in sterol biosynthesis, including the conversion of zymosterol to ergosterol[49]. During this process, SAM is converted to *S*-adenosylhomocysteine (SAH) and then recycled to L-homocysteine *via*

Sah1[50]. SAM is also diverted into polyamine spermidine synthesis, with intermediates capable of recycling back into L-methionine. These pathways are the main competing sinks that restrict SAM availability. Previous studies show that restricting transmethylation flux significantly increases intracellular SAM[51], and disruption of the polyamine pathway can further enhance SAM pools. Building on these insights, we targeted specific SAM-consuming pathways to increase SAM levels and decrease metabolic burden. This approach alleviates methionine feedback inhibition and enhances methylation capacity for downstream processes engineering. The synthesis of ergosterol is regulated by a coordinated set of ERG genes (*ergX*) [52], which are involved in cell growth and are generally classified as essential or nonessential. Essential genes are required for survival, while nonessential genes might be unnecessary during normal growth conditions. Both *ERG4* and *ERG6* are nonessential genes, but according to previous reports, deletion of *ERG6* (*Δerg6*) increases cellular susceptibility to stress-induced death[53]. In this study, instead of deleting *ERG6* and *ERG4*, we reduce their expression by replacing their native promoters with the weak promoter *HXT1*. This approach enabled a controlled reduction of ergosterol biosynthesis while avoiding the severe growth defects usually linked to complete gene deletions.

Another gene that may consume precursor amino acids is *SPE2*, which encodes *S*-adenosylmethionine decarboxylase, and can degrade SAM[54], a key enzyme in the polyamine biosynthesis pathway converts SAM into decarboxylated SAM, which is then used for spermidine and spermine production. This reaction is one of the major competing pathways for intracellular SAM. To reduce SAM diversion into polyamine production and increase its availability for EGT biosynthesis, we downregulated *SPE2* by replacing its native promoter with the weak *HXT1* promoter. In strain ST4016, *ERG6*, *ERG4*, and *SPE2* were simultaneously downregulated by substituting their native promoters with the weak *HXT1* promoter, thereby limiting SAM consumption through both sterol and polyamine pathways, and that strain was named ST4019. To further maximize the metabolic flux toward EGT, multiple copies of *Nc-egt1* were integrated into the rDNA locus and *Cp-egt2* into the δ-locus of the ST4019 strain to construct the ST4021 strain. Quantitative analysis of the transcriptional profiles revealed a significant correlation between integration strategy and expression levels. The relative expression levels of *Egt1* and *Egt2* in ST4016 were 10.9-fold and 8.6-fold of those in the reference single-copy integration strain (Figure 3C). In the further optimized strain ST4021, these levels were dramatically elevated to 22.5-fold for *Egt1* and 27.2-fold for *Egt2* relative to the single-copy control. Consequently, the expression levels in ST4021 were approximately 2.1-fold (*Egt1*) and 3.2-fold (*Egt2*) higher than those observed in ST4016. Based on these relative transcript abundances under shake-flask fermentation conditions, we estimated that the gene copy numbers for *Egt1* and *Egt2* were approximately 11 and 9 in ST4016, 23 and 28 in ST4021, respectively. Strain ST4021 accumulated 211.2 mg/L extracellular and 101.6 mg/L intracellular with a total of 312.8 mg/L of EGT (Figure 3B and 3D). Compared to the ST4016 strain, the ST4021 strain demonstrated a substantial enhancement in production performance, with extracellular EGT titers increasing by 39.1% and intracellular levels by 22.0%. These data underscore the efficiency of combining targeted metabolic sink attenuation with high-copy-number pathway integration to overcome SAM availability limitations and drive high-level EGT biosynthesis.

2.4 Medium optimization with supplementation of precursor amino acids

To increase the production of EGT, four different amino acids of Met, His, Cys, and Arg were supplemented to the culture medium as essential precursors for the synthesis of EGT

(Figure 4). Group A acted as the low-concentration control to determine the baseline impact of precursor amino acid supplementation on EGT production. Group B was set up to assess whether a slight increase in precursor levels would result in a noticeable boost in EGT yield. Group C aimed to balance the levels of methionine and histidine with those of cysteine and arginine, thereby testing a moderate-to-high concentration range to determine whether elevated levels of specific amino acids could promote EGT biosynthesis. Group D was selected as a high-concentration test to determine whether the increasing supply of methionine would substantially boost EGT production. Group E involved the application of very high levels of all precursor amino acids in an attempt to achieve even greater EGT accumulation, although such elevated concentrations may impose metabolic stress or lead to nutrient imbalance. Group F tested the effects of high concentrations of all precursor amino acids, under the hypothesis that extreme supplementation could result in oversaturation or cytotoxicity, thereby limiting yeast growth and consequently constraining EGT production.

The best formulation for EGT production belonged to Group D (Figure 4), which had a final concentration of 20 g/L of Met and 8 g/L of His, Cys, and Arg, respectively. This combination of amino acids was optimal for enhancing metabolic flux toward EGT biosynthesis, but higher concentrations led to diminishing returns or metabolic limitations. These results provide valuable information for further optimizing fermentation conditions for large-scale, environmentally friendly production of EGT.

2.5 Fed batch fermentation for EGT production

To further improve the production of EGT, the strain ST4021, which produced the highest EGT titer in flask fermentation, was cultured in a 5-L bioreactor with the addition of precursor amino acids. The initial glucose concentration was 50 g/L. The concentrations for precursor amino acids are 20 g/L MET and 8 g/L His, Cys, and Arg, which were used in the fermentation process. Glucose was added every 24 hours to boost the concentration by about 10 g/L each cycle. The fermentation was performed for 168 hours, at which the maximum OD_{600} value of fermentation broth reached 93.9, and EGT titer reached 969 mg/L extracellular and 342 mg/L intracellular, with total production of 1 312.2 mg/L, and productivity was calculated as 7.8 mg/(L·h) (Figure 5). These results highlight that combining controlled oxygen flux, antioxidant supplementation, and precise precursor feeding at optimal temperature and pH synergistically enhances EGT biosynthesis, providing a robust strategy for scale-up production.

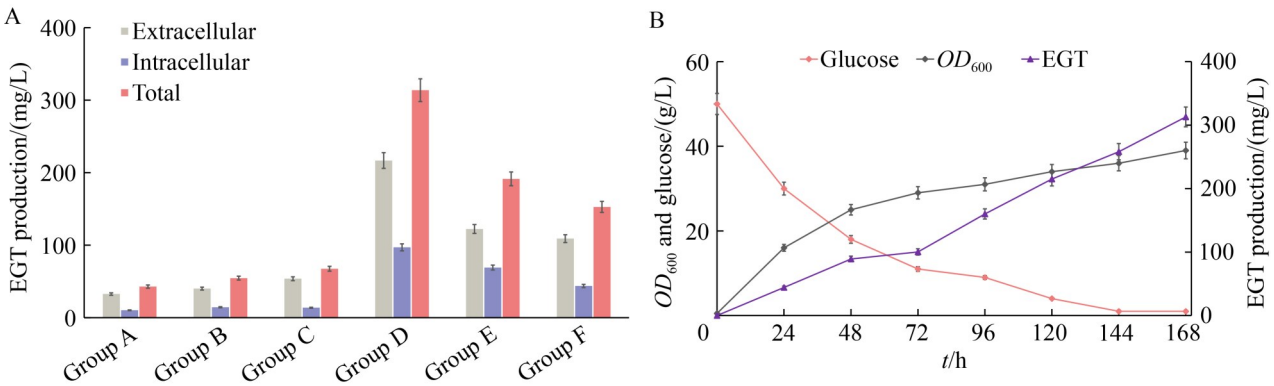

Figure 4 Medium optimization with different precursor amino acids concentration. A: The effects of different concentrations of Met, His, Cys, and Arg on EGT production; B: The flask fermentation process of Group D.

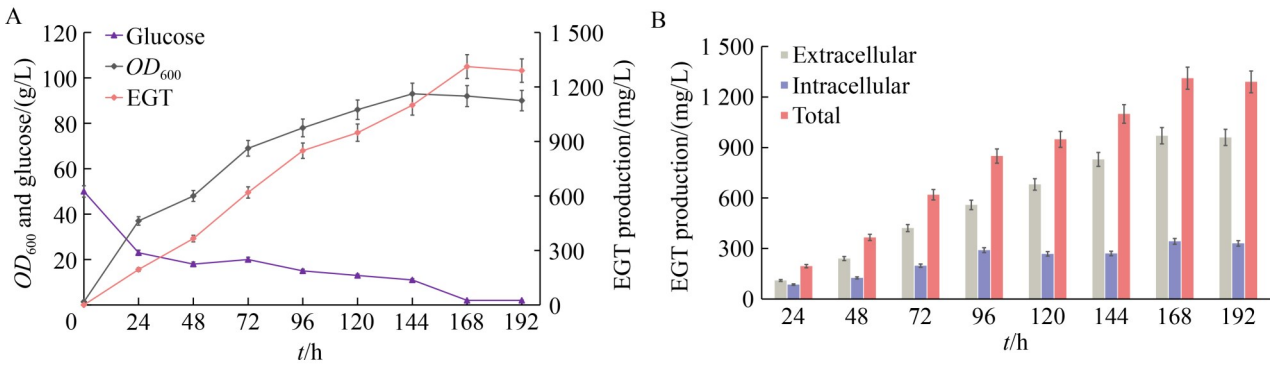

Figure 5 Fed-batch fermentation for EGT production by strain ST4021 using a 5-L bioreactor. A: The process of fed-batch fermentation; B: The accumulation of extracellular and intracellular EGT during fed-batch fermentation.

3 Discussion and conclusion

In this study, a high-level EGT production in *S. cerevisiae* was achieved by implementing a multi-layered metabolic engineering framework. This strategy involved screening heterologous biosynthetic enzymes, improving the supply of sulfur and precursor amino acids, reducing the activity of competing SAM-consuming pathways, and optimizing gene dosage *via* multi-copy integration. The final engineered strain ST4021 produced 312.8 mg/L EGT in shake flask fermentation and 1 312.2 mg/L in fed-batch fermentation, demonstrating the effectiveness of the combined metabolic engineering strategies.

The initial screening of eight EGT pathway variants revealed that enzyme origin and pairing critically influence pathway performance. The bimodular combination of *Ncegt1* from *N. crassa* with *Cpegt2* from *C. purpurea* in strain ST4006 yielded the highest EGT titer of 56.0 mg/L. Conversely, the bacterial-fungal hybrid strain incorporating *MsegtE* showed only moderate productivity (19.9 mg/L), consistent with reports that cross-kingdom enzyme combinations may suffer from incompatible catalytic mechanisms[37].

EGT biosynthesis involves three methylation steps mediated by *Egt1*, making SAM availability a key bottleneck for metabolic flux. In *S. cerevisiae*, the cell's internal SAM pool is carefully controlled and significantly affected by internal metabolic processes[45]. To overcome this limitation, methylenetetrahydrofolate reductase (MTHFR) engineering has been employed to enable continuous homocysteine remethylation through methyl tetrahydrofolate (CH_3-THF)[49], while the utilization of cost-effective one-carbon compounds[55] and the overexpression of *SAM2*[56] have also been shown to boost intracellular SAM levels. Overexpression of *SAM2* alone in strain ST4009 increased EGT production by 45.9% compared to ST4006 (from 56.0 to 81.7 mg/L), confirming that methyl donor availability is a primary constraint. The subsequent overexpression of *CYS3* and *HIS1* in strain ST4011 doubled the EGT production relative to ST4009, reaching 163.0 mg/L, demonstrating that histidine and cysteine limitations become exposed once the SAM supply is increased. Significantly, the most substantial improvement occurred when we concurrently strengthened the methionine-SAM axis (*MET6*, *STR2*, and *SAM2*) and ATP regeneration (*ADK1*) in strain ST4016, achieving 235.1 mg/L. This result is consistent with earlier co-expression approaches that involved *MET6* and *SAM2*[57]. These findings indicate that SAM availability depends on a coordinated system involving precursor supply, sulfur flux, and bioenergetics, rather than being limited by a single enzymatic bottleneck. The improved performance of strain ST4016 compared to earlier strains shows that simultaneously enhancing methionine regeneration and adenylate homeostasis more effectively increases methylation capacity than just

overexpressing *SAM2*. This is consistent with findings that maintaining a high SAM biosynthetic pool is essential to sustain high-flux EGT production[58].

The biosynthesis of ergosterol (*via ERG4* and *ERG6*) and polyamines (*via SPE2*) constitutes significant endogenous sinks for SAM. It has been demonstrated that the deletion of *SPE2* in *S. cerevisiae* substantially enhanced EGT. However, this change led to spermidine and pantothenate auxotrophy, requiring careful attention to supplementation[58]. Similarly, the deletion of *metJ* in *E. coli* alleviated the repression of methionine biosynthesis, achieving an EGT yield of 1.3 g/L, although they observed growth defects in the knockout strain[38]. In contrast, our promoter attenuation strategy using the weak *HXT1* promoter achieved partial flux redistribution without compromising vital functions. The strain ST4021 exhibited an increased EGT production without any apparent growth impairments, confirming this method as a practical alternative to gene knockout for industrial applications.

With a shake flask titer of 312.8 mg/L, strain ST4021 demonstrates competitive performance compared with previously reported yeast-based systems. This titer exceeds the EGT titer reported in *Y. lipolytica*, *R. toruloides*, and *E. coli* before fed-batch optimization[59-60]. It also compares favorably with the 106 mg/L achieved in the early-stage engineered *S. cerevisiae* strain before the comprehensive precursor engineering and medium optimization, which ultimately yielded 2.4 g/L in fed-batch[58]. Scaling up to 5-L fed-batch fermentation confirmed the industrial potential of strain ST4021, achieving 1 312.2 mg/L EGT over 168 hours with a productivity of 7.8 mg/(L·h). However, comparison with the most recent advancements highlights significant opportunities for optimizing the process. It was achieved an EGT concentration of 9.3 g/L in *Y. lipolytica* through a combination of metabolic and enzyme engineering, specifically utilizing TrEgt1 mutations (Y786A-A492V) alongside modular precursor pathway enhancement, resulting in a productivity of 55.4 mg/(L·h)[43]. 7.2 g/L EGT was achieved in *E. coli* by employing a betaine-driven methyl supply system and an inorganic sulfur module (Table 3)[61]. Similarly, it was attained 7.3 g/L in *Y. lipolytica* using multicopy integration tools (YaliCMulti/YaliHMulti)[42]. More recently, it was demonstrated that integrating membrane permeability engineering with Tregt2 enzyme engineering (E155C mutation) and copy number optimization resulted in a yield of 4.1 g/L in *E. coli* within 96 hours[62]. These comparisons suggest that although the strain design presented here is competitive at the shake flask level, the fermentation process itself necessitates systematic optimization to fully realize its production potential.

Throughout the engineering process, a substantial fraction of the produced EGT remained intracellular, with extracellular titers consistently 1.5-to 2-fold higher than intracellular levels. This distribution suggests active export; however, the persistent intracellular pool indicates that native yeast transporters have a limited capacity for EGT secretion. This phenomenon has been observed across various hosts. For instance, it was reported that only 5% – 30% of the total EGT was secreted in their initial *S. cerevisiae* strains[33]. Similarly, it was found that recombinant *Corynebacterium glutamicum* strains required extended cultivation periods for EGT secretion, suggesting that export is a rate-limiting step[63]. Despite the absence of identified EGT-specific exporters in *S. cerevisiae*, the observed gradual extracellular accumulation during fermentation suggests the possibility of passive diffusion or low-affinity transport proteins. Recent findings indicate that the overexpression of *mfsT1* from *Mycolicibacterium neoaurum*, a putative EGT transporter, significantly increased production in *E. coli*[61]. Similarly, it was demonstrated that co-augmentation with *mfsT1* enhanced EGT production in *M. neoaurum*[64]. Future engineering strategies should consider the heterologous expression of well-characterized EGT transporters, potentially in conjunction with membrane permeability modifications. This approach is exemplified by the work that achieved improved EGT export through the deletion of Δ*waaF* and Δ*msbB* in *E. coli*[63].

Table 3 Summary of EGT bioproduction in various microbial hosts

Hosts	Key metabolic engineering features	EGT titer (shake flask)	EGT titer (bioreactor)	Fermentation time	Feeding strategy	References
E. coli	Construction of a combined fungal-bacterial pathway (Tr*Egt1*/Tr*Egt2*+Ms*EgtD*/Ms*EgtE*); enhancement of Cys biosynthesis (*cysE*); introduction of a methyl donor regeneration system	141.3 mg/L	2.5 g/L	134 h	Fed-batch with glucose and low-dose amino acid feeding (1 g/L each of His, Met, Cys)	[30]
E. coli	Heterologous expression of *egtBCDE* from *M. smegmatis*; reinforcement of γ-GC supply by thiosulfate feeding	24.0 mg/L	−	72 h	Batch with His, Met, and thiosulfate supplementation	[31]
S. cerevisiae	Screening of fungal/bacterial EGT pathway combinations; expression of *NcEgt1* and *CpEgt2*; medium optimization; nitrogen metabolism engineering	80.0 mg/L	598.0 mg/L	84 h	Fed-batch with glucose, and supplementation of Arg, His, Met, and pyridoxine	[33]
S. cerevisiae	Heterologous expression of *Gfegt1* and *Gfegt2* from *G. frondosa*; optimization of carbon source (glycerol)	20.6 mg/L	−	168 h	Daily addition of 1% glycerol to the culture medium	[34]
E. coli	Heterologous expression of *Mp_egtB* from *M. pseudosasicola* with *egtDE* from *M. smegmatis* in a high Cys-producing, SAM-reinforced strain (CHΔmetJ)	657.0 mg/L	598.0 mg/L	192 h	Batch culture in Erlenmeyer flasks with His, Met, and Cys supplementation; no feeding.	[37]
E. coli	High Cys-producing strain; expression of *egtABCDE* from *M. smegmatis*; disruption of *metJ*; supplementation of precursors	275.0 mg/L	1.3 g/L	216 h	Fed-batch with glucose, Met, His, and thiosulfate feeding	[38]
E. coli	Enzyme engineering of methyltransferase (*EgtD*) and sulfoxide synthase (*NcEgt1*) *via* semi-rational design and random mutagenesis; high-throughput screening using ergothionase	290.0 mg/L	5.4 g/L	96 h	Fed-batch with glycerol and amino acid supplementation (24 g/L each of His, Met, Cys)	[41]
Y. lipolytica	Development of multi-copy integration tools (YaliCMulti/YaliHMulti) using LTRs and rDNA; multi-copy integration of *Egt1*/*Egt2*	432.0 mg/L	7.3 g/L	168 h	Fed-batch with glucose in 5 L fermenter	[42]
Y. lipolytica	Enzyme engineering of Tregt1 (Y786A-A492V); modular engineering of precursor pathways (sulfur assimilation, Met, His, Cys); knockout of *SPE2*	516.3 mg/L	9.3 g/L	168 h	Fed-batch with glucose and Met supplementation (20 g/L) and BHT antioxidant	[43]

(To be continued)

(Continued Table 3)

Hosts	Key metabolic engineering features	EGT titer (shake flask)	EGT titer (bioreactor)	Fermentation time	Feeding strategy	References
S. cerevisiae	Engineering of precursor supply (His overproduction, *MET14*, Δ*spe2*); deletion of SAM-competitive pathway (Δ*erg4*); medium optimization with pantothenate	106.2 mg/L	2.4 g/L	160 h	Fed-batch with glucose; no amino acid precursor supplementation	[58]
Y. lipolytica	Heterologous expression of *Ncegt1* and *Cpegt2*; phosphate-limitation strategy for biomass control	205.0 mg/L	1.6 g/L	220 h	Phosphate-limited fed-batch with glucose as the only carbon source	[59]
R. toruloides	Establishment of CRISPR-assisted Cre recombination (CACR) for iterative genome editing; overexpression of endogenous *Rtegt1*/*Rtegt2*; SAM pathway rebalancing (ADO1); high-throughput screening	267.4 mg/L	–	168 h	Batch with Met supplementation (2 g/L)	[60]
E. coli	Reconstruction of betaine-driven methyl supply system (*TnBHMT*, *SAM2*, *SAHase*, *ADO1*); inorganic sulfur supply module (*Egt1*, *EgtD*, *EanB*); enhancement of His biosynthesis (*hisG* mutant, operon amplification); deletion of *metJ*; overexpression of *mfsT1* transporter	1.2 g/L	7.2 g/L	96 h	Fed-batch with glycerol, betaine, and thiosulfate; no exogenous Met or Cys supplementation	[61]
E. coli	Membrane permeability engineering (Δ*waaF*, Δ*msbB*); protein engineering of *Tregt2* (E155C); copy number optimization of pathway genes; precursor (*sdaA*, *metJ*) and transporter engineering	334.2 mg/L	4.1 g/L	96 h	Fed-batch with glucose and amino acid feed (16 g/L Cys, 10 g/L Met, 10 g/L His)	[62]
C. glutamicum	Heterologous expression of *egtABCDE* and *egtBCDE* from *M. smegmatis*; expression of *egtB* from *M. pseudosasicola*/*M. brachiatum* with *egtDE* from *M. smegmatis* in L-Cys-producing strain (*CYS-2*)	100.0 mg/L	100.0 mg/L	336 h (batch)/ 120 h (fed-batch)	Fed-batch with glucose and ammonium sulfate; no exogenous His/Met supplementation required	[63]

(To be continued)

(Continued Table 3)

Hosts	Key metabolic engineering features	EGT titer (shake flask)	EGT titer (bioreactor)	Fermentation time	Feeding strategy	References
E. coli	Protein engineering of *Tr1* and *Tr2* *via* solubility tag fusion and truncation; knockout of competing pathways; overexpression of feedback-resistant *cysE*; copy number optimization of *cysM*; knockout of *pykA*, *yjeH*, and *purR*; overexpression of *metK* and *C. glutamicum*-derived *hisG*	430.9 mg/L	2.3 g/L	80 h	Fed-batch with glucose and amino acid feed (1 g/L betaine, 2 g/L each of His, Met, Cys, 0.1 g/L VB6, 0.001 g/L VB12)	[65]
B. licheniformis	Heterologous expression of *EanA*/*EanB* from *C. limicola*; expression of novel methyltransferase (*EanAN*) and sulfurtransferase (*EanBN*) from *B. bacterium* and *A. alkalidiazotrophicus*, respectively; whole-cell catalysis	643.8 mg/L	−	140 h	Exogenous addition of His, Met, and Cys (10 g/L each) using whole-cell transformation	[66]
C. glutamicum	Heterologous expression of *egtBCDE* from *M. smegmatis* in an L-Cys-producing strain (*CYS-2*); introduction of *egtB* from *Methylobacterium spp.* with *egtDE* from *M. smegmatis*; engineering of His and SAM biosynthesis; osmotic pressure modulation	267.0 mg/L	459.0 mg/L	336 h	Fed-batch with glucose and ammonium sulfate; no exogenous Met/His addition required	[67]
E. coli	Heterologous expression of *Tregt1* and *Tregt2* from *T. reesei*; co-expression of NcEgt1 and NcEgt2 from *N. crassa*	70.6 mg/L	4.3 g/L	143 h	Fed-batch with glucose and continuous feeding of amino acid mixture (40 g/L each of His, Met, Cys)	[68]
S. cerevisiae	Overexpression of *STR2*, *CYS3*, *MET6*, *SAM2*, *HIS1*, and *ADK1*, combined with downregulation of *ERG6*, *ERG4*, and *SPE2*, and multicopy integration of *Ncegt1* and *Cpegt2*	312.8 mg/L	1.3 g/L	168 h	Fed-batch fermentation with glucose as the primary carbon source, His, Met, Cys, and Arg were supplemented to the initial culture	This study

In conclusion, this study provides a comprehensive framework for resolving the multifaceted metabolic constraints associated with EGT production in yeast. By addressing enzyme selection, precursor supply, methyl donor availability, competing pathways, and gene dosage, we improved yields from 56.0 mg/L to 312.8 mg/L in shake flasks and 1 312.2 mg/L in fed-batch fermentation. Our shake flask titer is competitive among yeast systems; optimizing fermentation—

especially the feeding strategy, precursor dynamics, and process control—is crucial for further improvement. The engineering framework we developed, which includes pathway screening, precursor reinforcement, competition reduction, and multicopy integration, can be applied to optimize other SAM-dependent or amino acid-derived biosynthetic pathways in yeast.

Credit authorship contribution statement

Salman Khan: Designed the study, drafted the manuscript, and performed the majority of the experiments; LI Xiaoxiao: Conducted data analysis; YANG Qun: Conducted data analysis; ZHAO Yunying: Supervised the project, revised the manuscript, and provided funding; DENG Yu: Supervised the project, revised the manuscript, and provided funding.

Declaration of Competing Interest

The authors declare no competing financial interest.

References

[1] Kalaras MD, Richie JP, Calcagnotto A, Beelman RB. Mushrooms: a rich source of the antioxidants ergothioneine and glutathione[J]. Food Chemistry, 2017, 233: 429-433.
[2] Tanret C. The new base drawn from rye ergot, ergothioneine[J]. Comptes Rendus Hebdomadaires des Séances de l'Académie des Sciences, 1909, 25: 222-224.
[3] Halliwell B, Cheah IK, Tang RMY. Ergothioneine: a diet-derived antioxidant with therapeutic potential[J]. FEBS Letters, 2018, 592(20): 3357-3366.
[4] Pfeiffer C, Bauer T, Surek B, Schömig E, Gründemann D. Cyanobacteria produce high levels of ergothioneine[J]. Food Chemistry, 2011, 129(4): 1766-1769.
[5] Melville DB, Genghof DS, Inamine E, Kovalenko V. Ergothioneine in microorganisms[J]. Journal of Biological Chemistry, 1956, 223(1): 9-17.
[6] Genghof DS. Biosynthesis of ergothioneine and hercynine by fungi and *Actinomycetales*[J]. Journal of Bacteriology, 1970, 103(2): 475-478.
[7] Qiu YB, Chen ZL, Su EZ, Wang LB, Sun L, Lei P, Xu H, Li S. Recent strategies for the biosynthesis of ergothioneine[J]. Journal of Agricultural and Food Chemistry, 2021, 69(46): 13682-13690.
[8] Cumming BM, Chinta KC, Reddy VP, Steyn AJC. Role of ergothioneine in microbial physiology and pathogenesis[J]. Antioxidants & Redox Signaling, 2018, 28(6): 431-444.
[9] Seebeck FP. *In vitro* reconstitution of mycobacterial ergothioneine biosynthesis[J]. Journal of the American Chemical Society, 2010, 132(19): 6632-6633.
[10] Dubost N, Ou B, Beelman R. Quantification of polyphenols and ergothioneine in cultivated mushrooms and correlation to total antioxidant capacity[J]. Food Chemistry, 2007, 105(2): 727-735.
[11] Cheah IK, Halliwell B. Could ergothioneine aid in the treatment of coronavirus patients[J]. Antioxidants, 2020, 9(7): 595.
[12] D'Onofrio N, Servillo L, Giovane A, Casale R, Vitiello M, Marfella R, Paolisso G, Balestrieri ML. Ergothioneine oxidation in the protection against high-glucose induced endothelial senescence: involvement of SIRT1 and SIRT6[J]. Free Radical Biology and Medicine, 2016, 96: 211-222.
[13] Nakamichi N, Nakayama K, Ishimoto T, Masuo Y, Wakayama T, Sekiguchi H, Sutoh K, Usumi K, Iseki S, Kato Y. Food-derived hydrophilic antioxidant ergothioneine is distributed to the brain and exerts antidepressant effect in mice[J]. Brain and Behavior, 2016, 6(6): e00477.
[14] Hseu YC, Vudhya Gowrisankar Y, Chen XZ, Yang YC, Yang HL. The antiaging activity of ergothioneine in UVA-irradiated human dermal fibroblasts *via* the inhibition of the AP-1 pathway and the activation of Nrf2-mediated antioxidant genes[J]. Oxidative Medicine and Cellular Longevity, 2020, 2020(1): 2576823.
[15] Markova N, Yarosh D, Smiles K, Karaman-Jurukovska N. The natural antioxidant L-ergothioneine is integral to the skin's defense against ultraviolet-induced oxidative damage[J]. Journal of the American Academy of Dermatology, 2009, 60(3): AB156.
[16] Butterfield DA, Halliwell B. Oxidative stress, dysfunctional glucose metabolism and Alzheimer disease[J]. Nature Reviews Neuroscience, 2019, 20(3): 148-160.
[17] Borodina I, Kenny LC, McCarthy CM, Paramasivan K, Pretorius E, Roberts TJ, van der Hoek SA, Kell DB. The biology of ergothioneine, an antioxidant nutraceutical[J]. Nutrition Research Reviews, 2020, 33(2): 190-217.
[18] Cheah IK, Ng LT, Ng LF, Lam VY, Gruber J, Huang CYW, Goh FQ, Lim KHC, Halliwell B. Inhibition of amyloid-induced toxicity by ergothioneine in a transgenic *Caenorhabditis elegans* model[J]. FEBS Letters, 2019, 593(16): 2139-2150.
[19] Smith E, Ottosson F, Hellstrand S, Ericson U, Orho-Melander M, Fernandez C, Melander O. Ergothioneine is associated with reduced mortality and decreased risk of cardiovascular disease[J]. Heart, 2020, 106(9): 691-697.
[20] Chen S, Ho KJ, Hsieh YJ, Wang LT, Mau JL. Contents of lovastatin, γ-aminobutyric acid and ergothioneine in mushroom fruiting bodies and mycelia[J]. LWT, 2012, 47(2): 274-278.
[21] Xu JZ, Yadan JC. Synthesis of L-(+)-ergothioneine[J]. The Journal of Organic Chemistry, 1995, 60(20): 6296-6301.
[22] Han YW, Tang XY, Zhang YT, Hu XC, Ren LJ. The current status of biotechnological production and the application of a novel antioxidant ergothioneine[J].

Critical Reviews in Biotechnology, 2021, 41(4): 580-593.
[23] Sao Emani C, Williams MJ, Wiid IJ, Hiten NF, Viljoen AJ, Pietersen RD, van Helden PD, Baker B. Ergothioneine is a secreted antioxidant in *Mycobacterium smegmatis*[J]. Antimicrobial Agents and Chemotherapy, 2013, 57(7): 3202-3207.
[24] Pluskal T, Ueno M, Yanagida M. Genetic and metabolomic dissection of the ergothioneine and selenoneine biosynthetic pathway in the fission yeast, *S. pombe*, and construction of an overproduction system[J]. PLoS One, 2014, 9(5): e105177.
[25] Vit A, Misson L, Blankenfeldt W, Seebeck FP. Crystallization and preliminary X-ray analysis of the ergothioneine-biosynthetic methyltransferase EgtD[J]. Acta Crystallographica Section F Structural Biology Communications, 2014, 70(5): 676-680.
[26] Goncharenko KV, Vit A, Blankenfeldt W, Seebeck FP. Structure of the sulfoxide synthase EgtB from the ergothioneine biosynthetic pathway[J]. Angewandte Chemie International Edition, 2015, 54(9): 2821-2824.
[27] Vit A, Mashabela GT, Blankenfeldt W, Seebeck FP. Structure of the ergothioneine-biosynthesis amidohydrolase EgtC[J]. ChemBioChem, 2015, 16(10): 1490-1496.
[28] Jones GW, Doyle S, Fitzpatrick DA. The evolutionary history of the genes involved in the biosynthesis of the antioxidant ergothioneine[J]. Gene, 2014, 549(1): 161-170.
[29] Khonde PL, Jardine A. Improved synthesis of the super antioxidant, ergothioneine, and its biosynthetic pathway intermediates[J]. Organic & Biomolecular Chemistry, 2015, 13(5): 1415-1419.
[30] Bello MH, Barrera-Perez V, Morin D, Epstein L. The *Neurospora crassa* mutant *Nc*Δ*Egt-1* identifies an ergothioneine biosynthetic gene and demonstrates that ergothioneine enhances conidial survival and protects against peroxide toxicity during conidial germination[J]. Fungal Genetics and Biology, 2012, 49(2): 160-172.
[31] Osawa R, Kamide T, Satoh Y, Kawano Y, Ohtsu I, Dairi T. Heterologous and high production of ergothioneine in *Escherichia coli*[J]. Journal of Agricultural and Food Chemistry, 2018, 66(5): 1191-1196.
[32] Takusagawa S, Satoh Y, Ohtsu I, Dairi T. Ergothioneine production with *Aspergillus oryzae*[J]. Bioscience, Biotechnology, and Biochemistry, 2019, 83(1): 181-184.
[33] Van der Hoek SA, Darbani B, Zugaj KE, Prabhala BK, Biron MB, Randelovic M, Medina JB, Kell DB, Borodina I. Engineering the yeast *Saccharomyces cerevisiae* for the production of L-(+)-ergothioneine[J]. Frontiers in Bioengineering and Biotechnology, 2019, 7: 262.
[34] Yu YH, Pan HY, Guo LQ, Lin JF, Liao HL, Li HY. Successful biosynthesis of natural antioxidant ergothioneine in *Saccharomyces cerevisiae* required only two genes from *Grifola frondosa*[J]. Microbial Cell Factories, 2020, 19: 164.
[35] Doyle S, Cuskelly DD, Conlon N, Fitzpatrick DA, Gilmartin CB, Dix SH, Jones GW. A single *Aspergillus fumigatus* gene enables ergothioneine biosynthesis and secretion by *Saccharomyces cerevisiae*[J]. International Journal of Molecular Sciences, 2022, 23(18): 10832.
[36] Fujitani Y, Alamgir KM, Tani A. Ergothioneine production using *Methylobacterium* species, yeast, and fungi[J]. Journal of Bioscience and Bioengineering, 2018, 126(6): 715-722.
[37] Kamide T, Takusagawa S, Tanaka N, Ogasawara Y, Kawano Y, Ohtsu I, Satoh Y, Dairi T. High production of ergothioneine in *Escherichia coli* using the sulfoxide synthase from *Methylobacterium* strains[J]. Journal of Agricultural and Food Chemistry, 2020, 68(23): 6390-6394.
[38] Tanaka N, Kawano Y, Satoh Y, Dairi T, Ohtsu I. Gram-scale fermentative production of ergothioneine driven by overproduction of cysteine in *Escherichia coli*[J]. Scientific Reports, 2019, 9: 1895.
[39] Zhang XY, Guan JY, Yang YQ, Zuo SC, Liu C, Wang PC. Construction of an *E. coli* cell factory for ergothioneine through SAM-cycle enhancement and pathway reconstruction[J]. Journal of Biotechnology, 2026, 410: 298-308.
[40] Chen J, Wang Y, Du G, Kang Z. Enhancement of ergothioneine synthesis in *Escherichia coli via* optimization of precursor supply and cell membrane permeability[J]. Journal of Food Science and Biotechnology, 2022, 41:43-52.
[41] Zhang LW, Tang JW, Feng MQ, Chen SX. Engineering methyltransferase and sulfoxide synthase for high-yield production of ergothioneine[J]. Journal of Agricultural and Food Chemistry, 2023, 71(1): 671-679.
[42] Liu MS, Wu JJ, Yue MY, Ning Y, Guan X, Gao S, Zhou JW. YaliCMulti and YaliHMulti: stable, efficient multi-copy integration tools for engineering *Yarrowia lipolytica*[J]. Metabolic Engineering, 2024, 82: 29-40.
[43] Hu LF, Zhou JW, Zhang CT, Xu S. Enhanced production of ergothioneine in *Yarrowia lipolytica* through combined metabolic and enzyme engineering[J]. ACS Agricultural Science & Technology, 2025, 5(4): 603-612.
[44] Alamgir KM, Masuda S, Fujitani Y, Fukuda F, Tani A. Production of ergothioneine by *Methylobacterium* species[J]. Frontiers in Microbiology, 2015, 6: 1185.
[45] Thomas D, Surdin-Kerjan Y. Metabolism of sulfur amino acids in *Saccharomyces cerevisiae*[J]. Microbiology and Molecular Biology Reviews, 1997, 61(4): 503-532.
[46] Thomas D, Rothstein R, Rosenberg N, Surdin-Kerjan Y. SAM2 encodes the second methionine *S*-adenosyl transferase in *Saccharomyces cerevisiae*: physiology and regulation of both enzymes[J]. Molecular and Cellular Biology, 1988, 8(12): 5132-5139.
[47] Chu J, Qian JC, Zhuang YP, Zhang SL, Li YR. Progress in the research of *S*-adenosyl-l-methionine production[J]. Applied Microbiology and Biotechnology, 2013, 97(1): 41-49.
[48] Naz S, Liu P, Farooq U, Ma HW. Insight into de-regulation of amino acid feedback inhibition: a focus on structure analysis method[J]. Microbial Cell Factories, 2023, 22: 161.
[49] Bhatia M, Thakur J, Suyal S, Oniel R, Chakraborty R, Pradhan S, Sharma M, Sengupta S, Laxman S,

Masakapalli SK, Bachhawat AK. Allosteric inhibition of MTHFR prevents futile SAM cycling and maintains nucleotide pools in one-carbon metabolism[J]. Journal of Biological Chemistry, 2020, 295(47): 16037-16057.

[50] Tan LZ, Zhang YH, Liu P, Wu YH, Huang ZY, Hu ZC, Liu ZQ, Wang YS, Zheng YG. System metabolic engineering modification of *Saccharomyces cerevisiae* to increase SAM production[J]. Bioresources and Bioprocessing, 2025, 12: 19.

[51] Tomitori H, Kashiwagi K, Asakawa T, Kakinuma Y, Michael AJ, Igarashi K. Multiple polyamine transport systems on the vacuolar membrane in yeast[J]. Biochemical Journal, 2001, 353(3): 681-688.

[52] Mirjalili S. Evolutionary Algorithms and Neural Networks: Theory and Applications[M]. Studies in Computational Intelligence, Volume, 780. Cham: Springer, 2019: 43-55.

[53] Sokolov SS, Galkina KV, Litvinova EA, Knorre DA, Severin FF. The role of *LAM* genes in the pheromone-induced cell death of *S. cerevisiae* yeast[J]. Biochemistry (Moscow), 2020, 85(3): 300-309.

[54] Hébert A, Casaregola S, Beckerich JM. Biodiversity in sulfur metabolism in hemiascomycetous yeasts[J]. FEMS Yeast Research, 2011, 11(4): 366-378.

[55] Lv YK, Chang JM, Zhang WP, Dong HY, Chen S, Wang X, Zhao AQ, Zhang S, Alam MA, Wang SL, Du CJ, Xu JL, Wang WG, Xu P. Improving microbial cell factory performance by engineering SAM availability[J]. Journal of Agricultural and Food Chemistry, 2024, 72(8): 3846-3871.

[56] Chen YW, Tan TW. Enhanced *S*-adenosylmethionine production by increasing ATP levels in baker's yeast (*Saccharomyces cerevisiae*)[J]. Journal of Agricultural and Food Chemistry, 2018, 66(20): 5200-5209.

[57] Chen HL, Wang Z, Wang ZL, Dou J, Zhou CL. Improving methionine and ATP availability by *MET6* and *SAM2* co-expression combined with sodium citrate feeding enhanced SAM accumulation in *Saccharomyces cerevisiae*[J]. World Journal of Microbiology and Biotechnology, 2016, 32(4): 56.

[58] Van der Hoek SA, Rusnák M, Wang GK, Stanchev LD, de Fátima Alves L, Jessop-Fabre MM, Paramasivan K, Jacobsen IH, Sonnenschein N, Martínez JL, Darbani B, Kell DB, Borodina I. Engineering precursor supply for the high-level production of ergothioneine in *Saccharomyces cerevisiae*[J]. Metabolic Engineering, 2022, 70: 129-142.

[59] Van der Hoek SA, Rusnák M, Jacobsen IH, Martínez JL, Kell DB, Borodina I. Engineering ergothioneine production in *Yarrowia lipolytica*[J]. FEBS Letters, 2022, 596(10): 1356-1364.

[60] Liu K, Xiang GD, Li LK, Liu T, Ke J, Xiong LB, Wei DZ, Wang FQ. Engineering non-conventional yeast *Rhodotorula toruloides* for ergothioneine production[J]. Biotechnology for Biofuels and Bioproducts, 2024, 17: 65.

[61] Yan JJ, Chen YH, Ma YY, Yang X, Yao YH, Zhao GP, Zhang YF. Efficient ergothioneine production through reconstruction of the methyl and sulfur supply systems in *Escherichia coli*[J]. Trends in Biotechnology, 2026, 44(2): 477-495.

[62] Ling JH, Chen R, Wang MH, Yan CX, Xia RM, Zhang LH. Integrating membrane permeability engineering and enzyme design for efficient production of ergothioneine in *E. coli*[J]. Journal of Agricultural and Food Chemistry, 2025, 73(24): 15225-15234.

[63] Hirasawa T, Shimoyamada Y, Tachikawa Y, Satoh Y, Kawano Y, Dairi T, Ohtsu I. Ergothioneine production by *Corynebacterium glutamicum* harboring heterologous biosynthesis pathways[J]. Journal of Bioscience and Bioengineering, 2023, 135(1): 25-33.

[64] Ding YX, Chen JW, Ke J, Hu FY, Wen JC, Dong YG, Wang FQ, Xiong LB. Co-augmentation of a transport gene *mfsT1* in *Mycolicibacterium neoaurum* with genome engineering to enhance ergothioneine production[J]. Journal of Basic Microbiology, 2024, 64(4): 2300705.

[65] Kang XY, Wang Y, Luo W. Enhancing ergothioneine production by combined protein and metabolic engineering strategies[J]. Journal of Agricultural and Food Chemistry, 2025, 73(15): 9234-9245.

[66] Liu Z, Xiao FX, Zhang YP, Lu JW, Li YR, Shi GY. Heterologous and high production of ergothioneine in *Bacillus licheniformis* by using genes from anaerobic bacteria[J]. Metabolites, 2025, 15(1): 45.

[67] Takahashi Y, Hirasawa T. Enhancement of ergothioneine production in *Corynebacterium glutamicum* by increasing osmotic pressure[J]. Applied Microbiology and Biotechnology, 2025, 109: 255.

[68] Chen ZH, He YZ, Wu XY, Wang L, Dong ZY, Chen XZ. Toward more efficient ergothioneine production using the fungal ergothioneine biosynthetic pathway[J]. Microbial Cell Factories, 2022, 21: 76.